AEM Accepted Manuscript Posted Online 27 October 2021
Appl Environ Microbiol doi:10.1128/AEM.01842-21

Antarctic polyester hydrolases degrade aliphatic and aromatic polyesters at moderate temperatures

Paula Blázquez-Sánchez[1,2], Felipe Engelberger[1,2], Jerónimo Cifuentes-Anticevic[3], Christian Sonnendecker[4], Aransa Griñén[1,2], Javiera Reyes[1,2], Beatriz Díez[3,5,6], Victoria Guixé[7], P. Konstantin Richter[8], Wolfgang Zimmermann[4] and César A. Ramírez-Sarmiento[1,2*]*

[1]Institute for Biological and Medical Engineering, Schools of Engineering, Medicine and Biological Sciences, Pontificia Universidad Católica de Chile, Av. Vicuña Mackenna 4860, 7820436, Santiago, Chile.

[2]ANID — Millennium Science Initiative Program — Millennium Institute for Integrative Biology (iBio), Santiago, 8331150 Chile

[3]Department of Molecular Genetics and Microbiology, School of Biological Sciences, Pontificia Universidad Católica de Chile, Av. Libertador Bernardo O'Higgins 340, 8331150, Santiago, Chile.

[4]Institute of Analytical Chemistry, Leipzig University, Johannisallee 29, 04103 Leipzig, Germany.

[5]Center for Climate and Resilience Research (CR)[2], Av. Blanco Encalada 2002, 8370449, Santiago, Chile.

[6]FONDAP Center for Genome Regulation (CGR), Av. Blanco Encalada 2085, 8370415, Santiago, Chile.

[7]Departamento de Biología, Facultad de Ciencias, Universidad de Chile, Las Palmeras 3425, 7800003, Santiago, Chile.

[8]Institute of Bioanalytical Chemistry, Center for Biotechnology and Biomedicine, Leipzig University, Deutscher Platz 5, 04103 Leipzig, Germany.

RUNNING TITLE

Characterization of an Antarctic polyester hydrolase

KEYWORDS

Polyethylene terephthalate (PET) | polyester hydrolases | plastic biodegradation | *Oleispira antarctica* | *Moraxella* sp. | Antarctica | psychrophilic enzymes

*Correspondence should be addressed to:

Wolfgang Zimmermann. Institute of Analytical Chemistry, Leipzig University, Johannisallee 29, 04103 Leipzig, Germany; +49 341 973-6171; wolfgang.zimmermann@uni-leipzig.de

César A. Ramírez-Sarmiento, Institute for Biological and Medical Engineering, Schools of Engineering, Medicine and Biological Sciences, Pontificia Universidad Católica de Chile, Av. Vicuña Mackenna 4860, 7820436, Santiago, Chile; +56 2 2354-1110; cesar.ramirez@uc.cl

ABSTRACT

Polyethylene terephthalate (PET) is one of the most widely used synthetic plastics in the packaging industry, and consequently has become one of the main components of plastic waste found in the environment. However, several microorganisms have been described to encode enzymes that catalyze the depolymerization of PET. While most known PET hydrolases are thermophilic and require reaction temperatures between 60°C to 70°C for an efficient hydrolysis of PET, a partial hydrolysis of amorphous PET at lower temperatures by the polyester hydrolase *Is*PETase from the mesophilic bacterium *Ideonella sakaiensis* has also been reported. We show that polyester hydrolases from the Antarctic bacteria *Moraxella sp.* strain TA144 (Mors1) and *Oleispira antarctica* RB-8 (OaCut) were able to hydrolyze the aliphatic polyester polycaprolactone as well as the aromatic polyester PET at a reaction temperature of 25ºC. Mors1 caused a weight loss of amorphous PET films and thus constitutes a PET-degrading psychrophilic enzyme. Comparative modelling of Mors1 showed that the amino acid composition of its active site resembled both thermophilic and mesophilic PET hydrolases. Lastly, bioinformatic analysis of Antarctic metagenomic samples demonstrated that members of the Moraxellaceae family carry candidate genes coding for further potential psychrophilic PET hydrolases.

IMPORTANCE

A myriad of consumer products contains polyethylene terephthalate (PET), a plastic that has accumulated as waste in the environment due to its long-term stability and poor waste management. One promising solution is the enzymatic biodegradation of PET, with most known

enzymes only catalyzing this process at high temperatures. Here, we bioinformatically identified and biochemically characterized an enzyme from an Antarctic organism that degrades PET at 25ºC with similar efficiency than the few PET-degrading enzymes active at moderate temperatures. Reasoning that Antarctica harbors other PET-degrading enzymes, we analyzed available data from Antarctic metagenomic samples and successfully identified other potential enzymes. Our findings contribute to increasing the repertoire of known PET-degrading enzymes that are currently being considered as biocatalysts for the biological recycling of plastic waste.

INTRODUCTION

Plastics are long-chain synthetic polymers mainly derived from petroleum-based monomers that are widely employed in modern-day applications, such as fibers for clothing and containers for liquids and foods (1). The low cost, malleability and durability of these polymers has led to the production of ~8,300 million tons of synthetic polymer resins and fibers between 1950 and 2015 (2). The global market for polyethylene terephthalate (PET) is growing and expected to reach 38 billion USD by 2023 (3).

PET waste mismanagement and its resistance to degradation has resulted in a serious threat for the environment (2). Although strategies for waste management and recycling of PET exist, such as thermo-mechanical (i.e. recirculation of plastic waste to produce lower-quality materials) and chemical recycling (i.e. degradation via chemical ester bond cleavage), only a fraction of PET waste is presently recycled (4).

In this context, the discovery of microbial PET-degrading enzymes (5, 6) has emerged as a promising biological approach for plastic recycling (7, 8). These polyester hydrolases are typically cutinases (EC 3.1.1.74) (8) that share a conserved α/β-hydrolase fold and a catalytic triad of amino acids (9). Most enzymes described to date have been derived from thermophilic bacteria and fungi (5, 10) with an optimum activity near the glass transition temperature of PET (~65ºC) where the polymer chains become more flexible and prone to enzymatic hydrolysis (11–13).

*Is*PETase, a PET hydrolase from the mesophilic bacterium *Ideonella sakaiensis* 201-F6 has been described to degrade PET with higher efficiency at lower temperatures (20°C to 40ºC) than thermophilic cutinases (14). However, the extent of PET degradation by *Is*PETase in this

temperature range remained limited compared to hydrolysis by its thermophilic counterparts at their optimum temperature (~65ºC) (15).

*Is*PETase has been further studied by several groups, describing that the molecular basis of its activity at moderate temperatures is due to an improved substrate binding at its shallow active site cleft due to the presence of unique residues that enhance PET binding and control active site flexibility (16–19). Importantly, rational design of its active site (17, 20, 21) and its thermostability (22, 23) guided by bioinformatic analysis of currently known PET hydrolases has resulted in up to 300-fold higher activities than the wild-type enzyme.

Most research has been primarily focused on the identification and characterization of thermophilic cutinases, limited information on other PET hydrolases active at moderate temperatures has been available. A polyester hydrolase from the marine bacterium *Pseudomonas aestusnigri* (24) has also been reported to exhibit limited hydrolytic activity on amorphous PET at 30°C, and variants obtained by rational mutagenesis were also able to release low amounts of MHET from bottle-grade PET. Recent bioinformatic analysis of proteome and metagenome databases has identified 853 potential polyester hydrolases from marine and terrestrial environments including 6 Antarctic enzymes. Among these, an enzyme from *Oleispira antarctica* RB-8 hydrolyzed the aliphatic polyester polycaprolactone (PCL) at room temperature (25).

Psychrophilic microorganisms are interesting candidates as a source of novel enzymes adapted to catalytic activity at low temperatures (26). Hypothesizing that cold-adapted enzymes from such organisms could degrade PET at similar temperatures than *Is*PETase and exhibit differences in residue composition of the active site when compared to thermophilic enzymes, we biochemically characterize two polyester hydrolases from *Oleispira antarctica* RB-8 (OaCut), a

114 psychrophilic oil-degrading bacterium isolated from Antarctic coastal seawater (27) that has
115 already been reported as a PCL hydrolase (25), and a *Moraxella sp.* strain TA144 (Mors1), a
116 bacterium isolated from Antarctic seawater with an optimum growth temperature of 25ºC (28).
117
118 RESULTS

119 **Mors1 and OaCut are polyester hydrolases active at moderate temperatures**

120 We analyzed the ability of two hydrolases from Antarctic-inhabiting bacteria, Mors1 and OaCut,
121 to degrade PCL and PET at moderate temperatures. To detect polyester hydrolysis activity of
122 OaCut and Mors1, plate clearing assays were performed with PCL. Overnight incubation at 25ºC
123 resulted in the formation of clearing zones around *E. coli* colonies overexpressing Mors1 and
124 OaCut in plates containing PCL (Figure 1 A-B). These enzymes were then recombinantly
125 expressed and purified (Figure S1) for enzyme activity and stability analyses.
126 The PCL-hydrolyzing activity of the two enzymes was compared by measuring the decrease in
127 turbidity of a PCL nanoparticle suspension. Mors1 completely clarified the suspension after a
128 reaction time of 3 min while OaCut decreased the turbidity by only 28% in this time (Figure 1C).
129 Analysis of Mors1 by nano differential scanning fluorimetry (nanoDSF) indicated an apparent
130 melting temperature (T_m) of 52.0ºC and an onset temperature for denaturation of 31.0ºC. OaCut
131 showed an apparent melting temperature T_m of 40.4ºC and an onset temperature for denaturation
132 of 34.8ºC (Table 1 and Figure S2). These values were similar to the T_m of the mesophilic
133 *Is*PETase (22) and other previously characterized psychrophilic enzymes from *O. antarctica* RB-
134 8, such as the esterase OLEAN_C09750 with a reported T_m of 45ºC (29).
135 Using an enzyme concentration of 4.0 µg/ml (0.13 µM) and a PCL nanoparticle concentration of
136 0.07 mg/ml, the optimum reaction temperature for PCL hydrolysis by Mors1 was determined as

137 25°C (Figure 1D). Mors1 also showed a thermal inactivation temperature (T_{50}) of 48.7 ± 0.1ºC
138 and lost 95% of its PCL-hydrolyzing activity at 50ºC (Figure 1E).
139 A screening of different reaction buffers showed that the highest PCL-hydrolyzing activity was
140 obtained with sodium phosphate and potassium phosphate buffers at pH 8.0. A further increase
141 of the activity by 20% was observed in the presence of 200 mM NaCl in the reaction mixture
142 (Figure S3). These results confirm previous reports on the effects of buffer composition and salts
143 on the activity of psychrophilic enzymes (29) and polyester hydrolases (30).
144

145 **Kinetic parameters of PCL hydrolysis by Mors1 are similar to *Is*PETase**

146 When we compared the kinetic parameters for PCL hydrolysis of Mors1 with *Is*PETase and
147 polyester-degrading thermophilic enzymes from *Thermomonospora curvata*, we observed that
148 both Mors1 and *Is*PETase showed a high PCL-hydrolyzing activity (Table 2).
149 Determination of the kinetic parameters for Mors1 and *Is*PETase (Figure S4) demonstrated that
150 their apparent hydrolysis rates (k_τ) and adsorption equilibrium constants (K_A) were in a similar
151 range, with *Is*PETase showing 8.5% higher apparent hydrolysis rate and a 38% higher adsorption
152 equilibrium constant for PCL (Table 2). Remarkably, both enzymes showed 13- to 16-fold
153 higher apparent hydrolysis rates and equal or higher adsorption equilibrium constants at 25 ºC
154 than their thermophilic counterparts near the melting temperature of PCL (60°C) (31, 32).
155

156 **Mors1 hydrolyzes amorphous PET films at moderate temperatures**

157 We further compared the ability of Mors1 and *Is*PETase to hydrolyze amorphous PET films at
158 25°C. After a reaction time of 24 h with 400 nM (11 µg/ml) Mors1 and with 100 nM (2.7 µg/ml)
159 *Is*PETase in 1 M potassium phosphate buffer pH 8.0, we observed a 0.59% and 0.46% weight

160 loss of the films for Mors1 and *Is*PETase, respectively (Figure 2A). These protein concentration
161 and buffer molarity conditions were found to be optimal for the PET hydrolase activity of Mors1
162 (Figure S5), the latter being required as the terephthalic acid released during the hydrolysis
163 reaction would considerably lower the pH and alter the enzyme activity otherwise (30). While
164 both enzymes released similar amounts of terephthalic acid (TPA) and mono(2-hydroxyethyl)
165 terephthalate (MHET), MHET was the main aromatic hydrolysis product of Mors1 at pH 8.0
166 whereas *Is*PETase produced mainly TPA (Figure S6). Lower concentrations of Mors1 or higher
167 concentrations of *Is*PETase resulted in a decreased weight loss of the PET films. Similar assays
168 with OaCut showed a lower weight loss of 0.4% compared to Mors1 (1.98%) after a reaction
169 time of 6 days at 25°C (Figure 2B).
170 Upon longer reaction times up to 10 days, Mors1 degraded 2.5% of the PET films (Figure 2C).
171 The surface of the transparent PET films treated with Mors1 for 10 days became opaque
172 indicating an erosion of the surface (Figure 2D). Analysis by scanning electron microscopy
173 indeed showed the occurrence of pits and grooves on the surface (Figure 2E and 2F). Similar
174 effects have previously been observed with other PET-hydrolyzing enzymes (15).
175

176 **The active site of Mors1 presents features from mesophilic and thermophilic PET-**
177 **hydrolyzing cutinases**

178 Once we established that Mors1 can hydrolyze amorphous PET films at moderate temperatures,
179 we compared the amino acid residue composition of its active site with the mesophilic *Is*PETase
180 and with thermophilic PET hydrolases. We generated a comparative model of Mors1 using
181 Rosetta3 (33) (Figure S7 and Table S1) and also performed a multiple sequence alignment
182 (MSA) of Mors1 against *Is*PETase (UniProtKB: A0A0K8P6T7), OaCut (UniProtKB: R4YL88),

183 *Thermobifida fusca* cutinase (TfCut2, GenBank: PZN61876.1) and the metagenomic leaf-branch
184 compost cutinase (LCC, UniProtKB: G9BY57).
185 Inspection of the MSA (Figure 3A) and the comparative model of Mors1 (Figure 3B) showed
186 that Mors1 exhibits features of both mesophilic and thermophilic PET hydrolases. While all
187 enzymes showed a strict conservation of the catalytic triad (S189, D234, H264 in Mors1) and of
188 a Tyr residue (Y121 in Mors1) important for the activity of these enzymes (Figure 3C)(17),
189 Mors1 contains an additional disulfide bond (C231-C266 in Mors1, DB2 in Figure 3B) located
190 near the Asp and His residues of the catalytic triad, which is also present in *Is*PETase (C203-
191 C239 in *Is*PETase, Figure 3A) and in other Type IIa and IIb enzymes, that has been shown to be
192 critical for its hydrolytic activity (17, 18).
193 The model of Mors1 also revealed a potential third disulfide bridge (C60-C109, DB1 in Figure
194 3B) absent in *Is*PETase, which may constitute an adaptation to low temperatures. Fluorescence
195 labelling of free cysteine thiol groups of Mors1 (34) and comparison against a control protein
196 having only one free cysteine suggest that only a small fraction of Mors1 proteins are partially
197 reduced (Figure S8), thus suggesting that Mors1 could indeed harbor three disulfide bonds. Alas,
198 we were unable to purify single or double mutants of these cysteine residues for further analysis.
199 While both Mors1 and *Is*PETase also shared the conservation of a Trp residue (W188 in Mors1
200 and W159 in *Is*PETase), which is substituted by His in thermophilic counterparts, Mors1 carried
201 a Phe residue (F265) that is conserved among PET hydrolases of thermophilic microorganisms
202 and is replaced by Ser in *Is*PETase (Figure 3A, C and D). Both of these residues have recently
203 been the target for protein engineering of *Is*PETase, leading to a double mutant of this enzyme
204 with improved activity by the addition of His and Phe residues typically found in thermophilic
205 cutinases (21). Furthermore, residues Y214 and Y242 present in Mors1 and in other homologous

206 sequences from psychrophilic organisms corresponded to Trp in all other enzymes, and to His in
207 thermophilic cutinases and Ser in *Is*PETase, respectively (Figure 3A, C and D). Residue Y242 is
208 highly relevant as structural data has indicated that its substitution by Ser (S214) in *Is*PETase
209 enables the wobbling of its W185 (Y214 in Mors1) that is important for catalysis (16–19).
210 In previous reports, the ability of *Is*PETase to degrade PET at moderate temperature has been
211 partly explained by its higher active site flexibility when compared to the thermophilic cutinases
212 (18). Thus, we explored the structural flexibility of Mors1 by molecular dynamics (MD)
213 simulations (Figure 3E). The analysis of several 100 ns MD trajectories of Mors1 showed an
214 overall increase in RMSF mostly in loop regions throughout the whole protein when compared to
215 *Is*PETase. Of particular interest are three regions that conform the active site and its
216 surroundings: 1) the β6-β7 loop (residues 212-222) where Y214 from subsite I is located, whose
217 equivalent residue in *Is*PETase (the wobbling W185) is crucial for stabilization of the substrate
218 via π–π interactions; 2) helix α4 and the loops β7-α4 and β8-α4 (residues 231-251) in Mors1,
219 where the catalytic aspartate is located (D234); and 3) an extended loop (17) composed by
220 residues 260-269, where the catalytic histidine is located (H264), and the beginning of helix α5
221 (residues 269-277).
222

223 **Identification of polyester hydrolases from Antarctic marine environments**

224 To identify further potential polyester hydrolases from Antarctic marine environments, we
225 assembled two marine metagenomes from Chile Bay (Greenwich Island) in Antarctica (NCBI:
226 Bioproject no. PRJNA421008) (35) using SPAdes (36): One was corresponding to a condition of
227 low productivity, based on the concentration of chlorophyll *a* (Low Chl*a*), and the second was
228 corresponding to a condition of high productivity during a phytoplankton bloom recorded in the

229 austral summer of 2014 in Chile Bay (High Chl*a*). Once we obtained all predicted proteins from
230 these metagenomes using Prodigal (37), we used the full-length amino acid sequence of Mors1
231 (UniProtKB P19833) as reference to identify homologs from these predicted Antarctic
232 metagenome proteins using BLASTP (38).
233 This analysis led to the identification of 6 enzymes having 71-90% sequence identity and 56-
234 97% sequence coverage in both metagenomes (Table S2 and Figure 4). When analyzing the
235 source contigs, we observed that the proteins with lower sequence coverage (mtgnm1, mtgnm3)
236 were truncated not by the presence of terminal codons, but because the contig was terminated
237 before a protein termination signal could be identified. Moreover, bioinformatic analysis using
238 SignalP (39) identified a signal peptide in 4 of these enzymes (mtgnm1, mtgnm3, mtgnm4,
239 mtgnm6), in consistency to what is observed for all characterized PET hydrolases to date.
240 Regarding the taxonomic affiliation of these enzymes, BLAST analysis against the RefSeq
241 protein database showed that they had high sequence identity (>82%) with proteins of the genus
242 *Psychrobacter* of the Moraxellaceae family (Table S3). The difference in the taxonomic
243 assignment of these enzymes to the genus *Psychrobacter* and not to the genus *Moraxella* could
244 be explained by a possibly erroneous sequence annotation of Mors1, which was taxonomically
245 classified using biochemical tests and not genome phylogeny analysis.
246 When evaluating the relative abundance of the taxa that potentially carry these sequences in the
247 Antarctic metagenomes, we determined that the *Moraxellaceae* family represented ~40% of the
248 total reads assigned as 16S rRNA genes in the Low Chla metagenome. Meanwhile, in the High
249 Chl*a* metagenome, the reads assigned to the *Moraxellaceae* family represented only ~3% of the
250 total. These values were in good agreement with those reported previously (40), where
251 Pseudomonadales (to which *Moraxella* and *Psychrobacter* genera belong) was the dominant

252 marine order in a low Chl*a* metagenome, and then Alteromonadales order dominated in a high
253 Chl*a* metagenome obtained during the phytoplankton bloom recorded in Chile Bay in 2014.
254 Using Bowtie2 (41), we determined that the Mors1 homologs recruit only 0.0005% and 0.0001%
255 of the total number of reads from the Low and High Chl*a* metagenomes, respectively. This low
256 abundance, compared to the relative abundance of 16S rRNA genes of the *Moraxellaceae* family
257 members, indicates that not all members of this family are carriers of these candidate enzymes.
258

259 DISCUSSION

260 We characterized two psychrophilic polyester hydrolases, Mors1 and OaCut from the Antarctic
261 bacteria *Moraxella sp.* TA144, and *Oleispira antarctica* RB-8, respectively, demonstrating their
262 ability to hydrolyze both aliphatic and aromatic polyester at moderate temperatures. Both
263 enzymes hydrolyzed the aliphatic polyester PCL and the aromatic polyester PET, with Mors1
264 showing a higher activity. While the degradation of PCL by OaCut has been reported previously,
265 an hydrolysis of PET has not been observed in a plate clearing assay (25).
266 The hydrolysis of PCL at 30ºC by a lipase from *Moraxella sp.* TA144 (MorEst) has also been
267 reported (42). A weight loss of 18% after 3 days of reaction was achieved in a mixture
268 containing 10 mg/ml of powdered PCL with 25 mg of enzyme and a further addition of 12 mg of
269 MorEst 24 and 48 h later. MorEst also hydrolyzed bis(2-hydroxyethyl) terephthalate and a PET
270 dimer, but a commercial PET sample was not hydrolyzed. Since the sequence of the enzyme was
271 not communicated, the identity of MorEst with Mors1 could not be determined.
272 It has been previously demonstrated that polyester hydrolases, for example the metagenomic
273 leaf-branch compost cutinase LCC or Tcur1278 and Tcur0390 from the thermophilic
274 actinomycete *Thermomonospora curvata* efficiently degraded PCL at a reaction temperature of

about 50ºC (13, 32). *Is*PETase has been described not to be able to degrade aliphatic polyesters such as polybutylene succinate and polylactic acid (21). In contrast, we found that *Is*PETase showed kinetic parameters similar to Mors1 hydrolyzing the aliphatic polyester PCL at pH 8.0 at a reaction temperature of 25°C. Mors1 showed a considerable higher PET-degrading activity than OaCut. Mors1 caused a weight loss of amorphous PET films and released PET hydrolysis products at optimum reaction conditions in the same range as the mesophilic *Is*PETase, demonstrating the ability of Antarctic psychrophilic enzymes to degrade PET. It is worth noting that the activity of *Is*PETase can be further increased by about 3-fold at pH 9.0 (14).

A classification of PET hydrolases based on their amino acid residue conservation in subsites I and II within the active site of these enzymes (17) enabled to categorize OaCut as a Type IIa enzyme due to its residue composition (L105, L106, W176, F256, F259 in subsite II). In contrast, Mors1 presented differences in both subsites (D153, Y214 in subsite I; V122, S123, W188, F265, S268 in subsite II), which impedes its unambiguous classification under any of the Type I, IIa or IIb categories. These results suggest that the composition of the active site of these polyester hydrolases is more diverse than previously considered.

Computational analysis of the sequence and structure of Mors1 suggested that its ability to hydrolyze PCL and amorphous PET at moderate temperatures is due to features that this enzyme shares with both thermophilic PET hydrolases and the mesophilic *Is*PETase. The presence of a disulfide bond near the active site, absent in thermophiles but equivalent to the one found in Type II enzymes (17) was a prominent indicator that Mors1 could also show polyester-hydrolyzing activity at moderate temperatures. In *Is*PETase, this disulfide bond compensates the increased structural flexibility of its active site while keeping the integrity of the catalytic triad. An opening of the disulfide bond decreased the V_{max} for the hydrolysis of *p*-nitrophenyl acetate

by almost 28% (18) and its replacement by alanine causing a T_m drop of 13.2ºC (17). Our MD simulations provided evidence that Mors1 also possesses a highly flexible active site, which could explain its activity at 25ºC. Our analysis suggested the presence of a further disulfide bond (C60-C109) in Mors1, which could also correspond to the stabilization strategy of psychrophilic and psychrotropic organisms to counterbalance the additional flexibility on the structure of their enzymes[34].

The increased flexibility of regions that contain both catalytic and substrate binding residues could be indicative of enthalpic-entropic tradeoffs to enable PET hydrolysis at moderate temperatures, as it has been shown for other cold-active enzymes (43). However, further docking experiments followed by MD simulations are required to analyze such tradeoffs in the active site of Mors1.

Reasoning that there could be more enzymes from Antarctic microorganisms catalyzing the hydrolysis of polyesters at moderate temperatures, and taking into account recent bioinformatic analysis of proteome and metagenome databases that identified 6 Antarctic enzymes among 853 potential PET hydrolases from marine and terrestrial environments (25), we performed a metagenomic analysis of Antarctic marine environments. The results provided evidence for the presence of further potential polyester hydrolases homologous to Mors1 with likely similar activities in Antarctic coastal waters, specifically in members of the family Moraxellaceae. Among 6 new enzymes identified with moderate to high identity to Mors1, we observed a localized sequence variability in regions near the active site residues, which suggested potential differences in their polyester-hydrolyzing activity. No homologous Antarctic enzymes were detected outside this family, which could be due to a specific niche inhabited by some members of the Moraxellaceae family. The low abundance of the enzyme sequences in Antarctic

321 metagenomes compared to the relative abundance of the Moraxellaceae family members in the
322 bacterial marine community suggests a possible niche function of members of this family in
323 using these hydrolases.

324 Although *Is*PETase and Mors1 catalyzed the hydrolysis of amorphous PET at moderate
325 temperatures, their hydrolysis rates remained low when compared to thermophilic cutinases at
326 higher temperatures. Due to the stiffness of the PET polymer below its glass transition
327 temperature above 60°C, an extensive degradation of PET cannot be expected at 25°C (44).
328 However, in applications requiring a limited hydrolysis of PET at moderate temperatures, for
329 example in laundry detergents for synthetic textiles (45), the Antarctic psychrophilic polyester
330 hydrolases have the potential to become valuable industrial biocatalysts in the future.

331 Determining the existence of metabolic pathways to assimilate PET degradation products in
332 Antarctic microorganism communities (46) could give further clues as to whether there is an
333 evolutionary adaptation of microorganisms to consume PET in the environment or if the ability
334 of the described enzymes to hydrolyze PET is rather due to their unusual broad substrate
335 specificity.

336 Our results established that Mors1 and OaCut are polyester hydrolases able to hydrolyze both
337 aliphatic and aromatic polyesters at moderate temperatures. Sequence comparison analysis
338 showed that the active site of Mors1 contained features of both the mesophilic *Is*PETase and
339 thermophilic enzymes. Metagenomic analysis of Antarctic seawater samples enabled the
340 identification of potential further PET hydrolases of the Moraxellaceae family, their abundance
341 in the marine community, and sequence variations. Altogether, our results describe an Antarctic
342 psychrophilic enzyme that degrades amorphous PET at moderate temperatures, furthering our

343 understanding of the sequence variations that have allowed the emergence of this catalytic
344 activity in nature.
345
346 MATERIALS AND METHODS
347 **Bioinformatic identification of OaCut and Mors1**

348 A BLAST (38) search against the UniProt Knowledgebase (UniProtKB (47)) was performed
349 using the amino acid sequence of *Is*PETase (UniProtKB A0A0K8P6T7) as a query, identifying
350 the sequences of OaCut (UniprotKB R4YKL9, 53% sequence identity) and Mors1 (UniProtKB
351 P19833, 45% sequence identity). N-terminal signal peptides and disordered regions were
352 removed using SignalP (39) and PrDOS (48), respectively.

353 **Protein expression and purification**

354 Codon-optimized genes encoding truncated Mors1 (residues 59-319) and OaCut (residues 47-
355 310) were synthesized (Genscript, Piscataway, NJ, USA), cloned into a pET28a vector (EMD
356 Biosciences, Madison, WI, USA) as NdeI/BamHI fragments and transformed into *Escherichia*
357 *coli* BL21(DE3). The bacteria were grown in kanamycin-supplemented Terrific Broth medium
358 (Thermo Fisher Scientific, Waltham, MA, USA). Upon reaching OD_{600} = 0.6, protein expression
359 was induced with 1 mM isopropyl β-D-1-thiogalactopyranoside (IPTG) and the bacterial culture
360 was further grown for 16 h at 14ºC. Cells were harvested by centrifugation and then lysed by
361 sonication in buffer containing 50 mM sodium phosphate pH 8.0, 200 mM NaCl and 8 M urea. A
362 cleared lysate was collected by centrifugation and loaded onto a Ni-Sepharose resin (HisTrap FF
363 crude, GE Healthcare Life Sciences, Pittsburgh, PA, USA). To remove urea, His-tagged protein
364 was dialyzed overnight at 4ºC and then loaded onto a HiLoad Superdex 200 prep grade size-
365 exclusion chromatography column (GE Healthcare Life Sciences) using an ÄKTA pure FPLC

366 (GE Healthcare Life Sciences). The purity of the preparations was confirmed by sodium dodecyl
367 sulfate-polyacrylamide gel electrophoresis (SDS-PAGE) (Figure S1). Protein concentration was
368 determined by the Bradford assay (49) (ROTI Quant, Carl Roth GmbH + Co. KG, Karlsruhe,
369 Germany).

370 **PCL plate clearing assays**

371 Polycaprolactone (PCL) nanoparticle suspension was prepared as previously described (32, 50,
372 51). Plate clearing assays were performed to preliminary ascertain if OaCut and Mors1 degrade
373 PCL (51). For the preparation of PCL agar plates, nanoparticle suspensions of PCL were added
374 to autoclaved LB-agar (6% v/v) at 60ºC supplemented with 0.5 mM IPTG and 37 µg/ml
375 kanamycin. Recombinant *E. coli* cells harboring the pET28a-OaCut and pET28a-Mors1 plasmids
376 were inoculated onto the plates and incubated at room temperature up to 4 days. The formation
377 of a clearing zone around colonies was used as indication of PCL-hydrolyzing activity (25).

378 **Thermal stability of OaCut and Mors1**

379 The apparent melting temperature (T_m) of OaCut and Mors1 was determined using nano-
380 differential scanning fluorimetry (nanoDSF, Prometheus NT.48, Nanotemper Technologies,
381 Munich, Germany). A thin glass capillary was filled with purified Mors1 and OaCut at a
382 concentration of 150 µg/ml in 20 mM HEPES pH 7.5, 70 mM NaCl, and heated from 20°C to
383 95ºC with a slope of 1°C/min (Figure S2). The intrinsic fluorescence emission of tryptophan
384 residues was measured at 330 and 350 nm, and the first derivative of the ratio of fluorescence at
385 330 and 350 nm was calculated to obtain the apparent T_m.

386 **Determination of optimum reaction temperature and buffer conditions for PCL hydrolysis**
387 **by Mors1**

388 To determine optimum reaction temperature and buffer conditions for the hydrolysis of PCL
389 by Mors1, the hydrolysis rates were determined by monitoring the decrease in turbidity of a PCL
390 nanoparticle suspensions as previously described (32, 52). The reaction mixtures contained
391 buffer and purified Mors1 (4.0 µg/ml) in a total volume of 200 µl. The reaction was started by
392 the addition of 0.07 mg/ml PCL nanoparticle suspension. Initial hydrolysis rates were determined
393 from the linear part of the graphs of decreasing OD_{600} over time. Experiments were performed in
394 triplicates. To determine the optimum reaction temperature for the hydrolysis of PCL by Mors1,
395 initial hydrolysis rates were measured at reaction temperatures between 5°C and 35°C in 20 mM
396 HEPES pH 7.5 every 6 seconds using a Cary 60 UV-Vis spectrophotometer (Agilent
397 Technologies, Santa Clara, CA, USA). To determine the optimum NaCl concentration for the
398 hydrolysis of PCL by Mors1, hydrolysis rates were measured in 20 mM HEPES pH 7.5 buffer
399 supplemented with NaCl in concentrations of 100, 200, and 500 mM. PCL hydrolysis rates were
400 determined after 1, 3 and 24 h of incubation at 25ºC. The enzyme activity determined after 1 h of
401 incubation in 20 mM HEPES pH 7.5 buffer was set to 100%.

402 The half-inactivation temperature of Mors1 (T_{50}), i.e., the temperature at which the enzyme
403 activity was reduced by 50% in relation to its activity at 25°C was determined by incubating 3.0
404 µg/ml Mors1 for 15 min in 125 mM sodium phosphate buffer pH 8.0 containing 200 mM NaCl
405 at temperatures from 20°C to 80ºC. The residual activity was determined at 25°C by measuring
406 the hydrolysis rates of PCL nanoparticles. The data were fitted to a sigmoidal Boltzmann
407 regression curve and the T_{50} value was obtained by determination of the inflection point.

408 The effect of five buffers (sodium phosphate, Bis-Tris, HEPES, Tris and potassium phosphate) at
409 pH 7.0 and 8.0 (Tris also at pH 9.0) on the hydrolysis of PCL nanoparticles by Mors1 was
410 compared by reacting 4.0 µg/ml Mors1 with 0.07 mg/ml PCL nanoparticles in 125 mM of the

411 corresponding buffer supplemented with 200 mM NaCl for 1, 3, and 72 h at 25º C. Hydrolysis
412 rates determined after 1 h in 20 mM HEPES pH 7.5, The enzyme activity determined at 200 mM
413 NaCl was set to 100%.

414 **Kinetic parameters of PCL hydrolysis by Mors1**

415 To determine the kinetic parameters of the PCL hydrolysis reaction catalyzed by Mors1 and
416 *Is*PETase, assays were performed at 25°C in a reaction mixture containing 125 mM sodium
417 phosphate pH 8.0, 200 mM NaCl and 0.07 mg/ml PCL nanoparticles with varying enzyme
418 concentrations from 0.6 to 22.0 µg/ml. Optimal buffer conditions for these assays (Figure S3)
419 were determined as described above. Assays were performed in triplicates using 96-well
420 microplates, measuring the change in turbidity at OD_{600} in 10 sec intervals for a total reaction
421 time of 10 min with a Synergy HTX multi-mode microplate reader (Biotek Instruments Inc,
422 Winooski, VT, USA). The kinetic parameters were determined with a pseudo-first order kinetic
423 equation (32, 52) (Figure S4).

424 **Hydrolysis of amorphous PET films by Mors1, OaCut, and *Is*PETase**

425 Amorphous PET films with a size of 0.5 cm × 3 cm (~45 mg) (250 µm thickness; product
426 number ES301445, Goodfellow, Hamburg, Germany) were incubated with 1 M potassium
427 phosphate pH 8.0, 200 mM NaCl and 400 nM of Mors1, 400 nM of OaCut and 100 nM of
428 *Is*PETase at 25ºC for 24 h with shaking. The PET films were collected, washed with water,
429 aqueous SDS (0.5%) and ethanol, dried at 50ºC overnight and weighted to determine the weight
430 loss gravimetrically. Hydrolysis reactions were also performed for 6, 7 and 10 days with 400 nM
431 Mors1 and for 6 days with 400 nM OaCut.

432 The soluble PET hydrolysis products mono(2-hydroxyethyl) terephthalate (MHET) and
433 terephthalic acid (TPA), present in the supernatants of 24 h reactions of the PET films with the
434 enzymes, were analyzed by HPLC using a C18 column (Eurosper II 100-5; 150 x 2 mm with pre-
435 column, Knauer Wissenschaftliche Geräte GmbH, Berlin, Germany) at a flow rate of 0.3 mL/min
436 on an Agilent 1100 Series HPLC instrument (Agilent Technologies, La Jolla, CA, USA). The
437 mobile phase consisted of acetonitrile with 0.1% formic acid (A) and 0.1% formic acid (B). A
438 gradient was performed as follows: 95% B (0.0 min), 80% B (0.1 min), 76% B (3.0 min), 60% B
439 (3.1 min), 0% (8.0 min), hold for 2 min and back to 95% B (analysis time 12.0 min). The
440 injection volume of the sample was 2 µL and the separated products were detected by their
441 absorbance at 241 nm. TPA (Sigma Aldrich, St. Louis, MO, USA) and MHET was used as
442 standard. MHET was synthetized as described elsewhere by the hydrolysis of bis(hydroxyethyl)
443 terephthalate (BHET) (Sigma Aldrich, St. Louis, MO, USA) with KOH (53). Trimesic acid
444 (TMA) (Sigma Aldrich, St. Louis, MO, USA) was used as internal standard. The amount of PET
445 film per microliter of the reaction volume (0.025 mg PET/µl reaction) was identical as described
446 for the analysis of *Is*PETase (14).

447 **Scanning electron microscopy of PET films**

448 PET films fixed on glass substrates were analyzed on a scanning electron microscope (EVO
449 LS10, Carl Zeiss GmbH, Germany) with a LAB6 cathode (Kimball Physics, New Hampshire,
450 USA) and a secondary electron detector. PET films were sputter-coated using a BAL-TEC model
451 SCD 050 (Leica Biosystems, Wetzlar, Germany) with 25 nm gold prior to imaging. Images were
452 captured at an acceleration voltage of 7kK and a probe current of 5pA.

453 **Comparative modelling of Mors1**

454 A comparative model for Mors1 was generated by first selecting high-sequence identity structure
455 templates through a BLAST search against the Protein Data Bank(54). The solved crystal
456 structures of *Is*PETase (PDB 6EQE)(21), the cutinases from *Thermobifida cellulosilytica* (PDB
457 5LUI)(55) and *Thermobifida fusca* (PDB 4CG2)(56) and a polyester hydrolase of *Pseudomonas*
458 *aestusnigri* (PDB 6SBN)(24) were selected.

459 Chain A of each structure was extracted and used as template alongside a RosettaScripts XML
460 modelling protocol(57) to generate a total of 1,000 models, where explicit information about the
461 position of the two conserved disulfide bonds and an additional bond were obtained according to
462 the cysteine residues present in the sequence. The lowest-energy model with the lowest RMSD
463 against the template structures was selected and its stereochemical quality was assessed using
464 Verify3D(58), PROVE(59), PROCHECK(60) and WHATCHECK(61). Further refinement of
465 this structure was conducted using two custom relax protocols(62) with and without restraints on
466 the active site, generating 5,000 additional models that underwent a similar energetical and
467 structural quality assessment for selection of a final model.

468 The five models with lowest-energy and RMSD against the template structure of *Is*PETase (PDB
469 6EQE) were selected for further analysis (Table S1 and Figure S7). We did not observe
470 significant differences in the Ramachandran plots for the models 119, 620, 650, 803 and 952.
471 Only 2 amino acids, excluding glycine, were in the non-favored regions, similar to the structure
472 of *Is*PETase who presented one residue in a non-favored region, corresponding to serine 132.

473 With Verify3D(58), which determines the compatibility of the model with its own primary
474 sequence based on known protein structures, we obtained positive values for all the models, with
475 models 119 and 650 showing the best results. With PROVE, better results were obtained for

476 model 952 with a buried outlier protein atom total of 3.6 %. Considering WHATCHECK results,
477 the model 199 showed less errors in comparison to the others and displayed a properly oriented
478 catalytic triad as in the template structures. Thus, model 119 was selected, and 5,000 relaxed
479 models were generated. No improvements were obtained, indicating a good quality of the model
480 119.

481 **Molecular dynamics simulations**

482 Molecular dynamic (MD) simulations with Mors1 and *Is*PETase (PDB 6EQE) were carried out
483 using AMBER16 along with the ff14SB force field (63). The protonation state of the residues at
484 pH 8.0 was estimated using the H++ server (64). Then, a system was solvated with TIP3P water
485 molecules and neutralized with counter ions in a truncated octahedral box of 1.5 nm of padding
486 with periodic boundary conditions. The system was first minimized using a steepest descent
487 method with position restraints on waters and ions, followed by a second minimization without
488 any position restraints. The system was heated from 0 to 298 K for 150 ps at a constant volume
489 using a Langevin thermostat, followed by equilibration of the solvent atoms of each system for 1
490 ns at 298 K and constant pressure of 1 bar using a Berendsen barostat until density was stable,
491 upon which a third and final equilibration step of the whole system for 1 ns under the same
492 temperature and pressure conditions was performed. Production MD runs were carried out in
493 four replicas for 100 ns each, using a timestep of 2.0 fs alongside the SHAKE (65) algorithm and
494 the particle mesh Ewald method(66) for long-range electrostatics, with a 10 Å cutoff for short-
495 range electrostatics. Independent runs were ensured by using random seeds for initial velocities
496 during the equilibration step. Replicas were checked for structural convergence using the overall
497 backbone root mean-square deviation (RMSD) from the first frame. RMSD and per-residue root
498 mean square fluctuations (RMSF) were calculated using CPPTRAJ of AmberTools20(67).

499 **Fluorescent dye labeling of free cysteines in Mors1**

500 The presence of free sulfhydryl groups of cysteine residues in Mors1 was determined by covalent
501 labeling with the fluorescent dye 7-fluoro-2,1,3-benzoxadiazole-4-sulfonamide (ABD-F) (34).
502 Both Mors1 and BSA were adjusted to equal molar concentrations and 4 µL of protein was
503 mixed with 5 µL of 2x reaction buffer (200 mM H3BO3, 4 mM EDTA, 6% SDS, pH 8.0), 1 µL
504 of 10x ABD-F (40 mM in DMSO) and incubated for 30 min at 37°C (Figure S8). Labeled
505 samples were separated on an SDS-PAGE gel under non-reducing conditions and fluorescence
506 was detected in a ChemiDoc XRS+ Gel Imaging System (Bio-Rad Laboratories, Hercules CA,
507 USA). BSA was used as a positive control since it contains 35 cysteine residues that form 17
508 disulfide bridges and one free cysteine which can be covalently labeled with ABD.

509 **Identification of potential PET hydrolases in Antarctic coastal metagenomes**

510 Genes encoding Mors1 homologs were identified from massive sequencing data obtained in
511 2014 from surface marine waters of Bahía Chile, Antarctica (35), available at the NCBI
512 Bioproject no. PRJNA421008. Metagenome readings were filtered using a quality score (Qscore)
513 > 30 and assembled with the SPAdes v3.10.1 software using the "meta" option (36). The
514 prediction of open reading frames (ORFs) was made from contigs greater than 500 bp with
515 Prodigal v2.6.3 using the “meta” mode and bypassing the Shine-Dalgarno sequence (37). Lastly,
516 potential polyester hydrolases from the predicted proteins of these metagenomes were identified
517 via local sequence homology analysis against the protein sequence of Mors1 (UniProtKB
518 P19833) using BLASTP (38), with hits having >50% coverage and >70% sequence identity
519 considered valid.

520 **Abundance and taxonomic affiliation of potential metagenomic PET hydrolases**

521 The composition of the bacteria community was evaluated through 16S miTAG analysis, which
522 were obtained and recorded from metagenomes using METAXA2 (68) in metagenomic mode
523 using default parameters. Recruitment of readings to the sequences of potential Mors1 homologs
524 was carried out through the use of Bowtie2 v2.2.6 (41) in the end-to-end alignment mode and
525 allowing 1 mismatch in a seed alignment during multiseed alignment. Then, we identified the
526 possible taxonomic identity of the candidate metagenome sequences through BLASTP (38)
527 against the Refseq_prot database (NCBI, January 2020). Only the best hit was reported, since the
528 first 10 results corresponded to the same taxonomy.

529 **Data availability**

530 The results from comparative modelling of Mors1 using Rosetta, MD simulations of *Is*PETase
531 and Mors1 and homologous metagenomic sequences identified from NCBI Bioproject no.
532 PRJNA421008 are available for download at the laboratory's simulation archive in the Open
533 Science Framework (OSF, https://osf.io/bn6u3/). The protein sequences of *Is*PETase, OaCut and
534 Mors1 are available at the UniProt KB under accession codes A0A0K8P6T7 (*Is*PETase),
535 R4YL88 (OaCut) and P19833 (Mors1).

536

537 AUTHOR CONTRIBUTIONS

538 PBS, BD, WZ, CARS: conceptualization. PBS, FE, JC, CS, BD, WZ, CARS: methodology.
539 PBS, FE, JC, AG, CS, KR, JR: investigation. PBS, FE, JC, BD, CARS: formal analysis. PBS,
540 FE, JC, BD, VG, WZ, CARS: writing – original draft. PBS, BD, VG, WZ, CARS: writing –
541 review & editing. PBS, CS, BD, VG, CARS: funding acquisition.

542

ACKNOWLEDGEMENTS

This research was funded by Instituto Antártico Chileno (INACH Regular Grant RG_47_16 to CARS and Doctoral Thesis Support Grant DG_11_18 to PBS), the National Agency for Research and Development (ANID) from Chile and the Sao Paulo State Foundation for Research (FAPESP) from Brazil (ANID-FAPESP PCI 2019/13259-9), and ANID – Millennium Science Initiative Program – ICN17_022. PBS and JR were funded by ANID Doctoral Scholarships (21191979 and 21191684, respectively). CS was funded by the Biotechnology and Biological Sciences Research Council (BB/T011289/1). BD was funded by DPI, grant number DPI20140044-ANID. Powered@NLHPC: This research was partially supported by the supercomputing infrastructure of the NLHPC (ECM-02).

We gratefully acknowledge Ronny Frank from the Centre for Biotechnology and Biomedicine, Molecular Biological-Biochemical Processing Technology of Leipzig University for providing the SEM images.

CONFLICT OF INTEREST

The authors declare no conflict of interest.

REFERENCES

1. Scott G. 2006. Polymers in modern life, p. 1–18. *In* Scott, G (ed.), Polymers and the Environment. RSC Publishing.
2. Jambeck JR, Geyer R, Wilcox C, Siegler TR, Perryman M, Andrady A, Narayan R, Law KL. 2015. Plastic waste inputs from land into the ocean. Science 347:768–771.
3. Satsangi S. 2017. Polyethylene Terephthalate (PET) Market by Application (Beverages, Sheet & Films, Consumer Goods, Food Packaging, and Others) and End-use Industry (Packaging, Electrical & Electronics, Automotive, Construction, and Others): Global Opportunity Analysis and Industry Forecast, 2017-2023.
4. Garcia JM, Robertson ML. 2017. The future of plastics recycling. Science 358:870–872.
5. Kawai F, Kawabata T, Oda M. 2019. Current knowledge on enzymatic PET degradation and its possible application to waste stream management and other fields. Appl Microbiol Biotechnol 103:4253–4268.
6. Taniguchi I, Yoshida S, Hiraga K, Miyamoto K, Kimura Y, Oda K. 2019. Biodegradation of PET: Current Status and Application Aspects. ACS Catal 9:4089–4105.
7. Zimmermann W. 2020. Biocatalytic recycling of polyethylene terephthalate plastic: Biocatalytic plastic recycling. Philos Trans R Soc A Math Phys Eng Sci 378:1–7.
8. Wei R, Zimmermann W. 2017. Biocatalysis as a green route for recycling the recalcitrant plastic polyethylene terephthalate. Microb Biotechnol 10:1302–1307.
9. Lenfant N, Hotelier T, Velluet E, Bourne Y, Marchot P, Chatonnet A. 2013. ESTHER, the database of the α/β-hydrolase fold superfamily of proteins: Tools to explore diversity of functions. Nucleic Acids Res 41:D423–D429.
10. Wei R, Zimmermann W. 2017. Microbial enzymes for the recycling of recalcitrant petroleum-based plastics: how far are we? Microb Biotechnol 10:1308–1322.
11. Ronkvist ÅM, Xie W, Lu W, Gross RA. 2009. Cutinase-Catalyzed hydrolysis of poly(ethylene terephthalate). Macromolecules 42:5128–5138.
12. Mueller RJ. 2006. Biological degradation of synthetic polyesters-Enzymes as potential catalysts for polyester recycling. Process Biochem 41:2124–2128.

13. Sulaiman S, Yamato S, Kanaya E, Kim J-J, Koga Y, Takano K, Kanaya S. 2012. Isolation of a Novel Cutinase Homolog with Polyethylene Terephthalate-Degrading Activity from Leaf-Branch Compost by Using a Metagenomic Approach. Appl Environ Microbiol 78:1556–1562.

14. Yoshida S, Hiraga K, Takehana T, Taniguchi I, Yamaji H, Maeda Y, Toyohara K, Miyamoto K, Kimura Y, Oda K. 2016. A bacterium that degrades and assimilates poly(ethylene terephthalate). Science 351:1196–1199.

15. Wei R, Breite D, Song C, Gräsing D, Ploss T, Hille P, Schwerdtfeger R, Matysik J, Schulze A, Zimmermann W. 2019. Biocatalytic Degradation Efficiency of Postconsumer Polyethylene Terephthalate Packaging Determined by Their Polymer Microstructures. Adv Sci 6:1900491.

16. Han X, Liu W, Huang J-W, Ma J, Zheng Y, Ko T-P, Xu L, Cheng Y-S, Chen C-C, Guo R-T. 2017. Structural insight into catalytic mechanism of PET hydrolase. Nat Commun 8:2106.

17. Joo S, Cho IJ, Seo H, Son HF, Sagong HY, Shin TJ, Choi SY, Lee SY, Kim KJ. 2018. Structural insight into molecular mechanism of poly(ethylene terephthalate) degradation. Nat Commun 9:382.

18. Fecker T, Galaz-Davison P, Engelberger F, Narui Y, Sotomayor M, Parra LP, Ramírez-Sarmiento CA. 2018. Active Site Flexibility as a Hallmark for Efficient PET Degradation by I. sakaiensis PETase. Biophys J 114:1302–1312.

19. Liu B, He L, Wang L, Li T, Li C, Liu H, Luo Y, Bao R. 2018. Protein Crystallography and Site-Direct Mutagenesis Analysis of the Poly(ethylene terephthalate) Hydrolase PETase from Ideonella sakaiensis. ChemBioChem 19:1471–1475.

20. Ma Y, Yao M, Li B, Ding M, He B, Chen S, Zhou X, Yuan Y. 2018. Enhanced Poly(ethylene terephthalate) Hydrolase Activity by Protein Engineering. Engineering 4:888–893.

21. Austin HP, Allen MD, Donohoe BS, Rorrer NA, Kearns FL, Silveira RL, Pollard BC, Dominick G, Duman R, El Omari K, Mykhaylyk V, Wagner A, Michener WE, Amore A, Skaf MS, Crowley MF, Thorne AW, Johnson CW, Woodcock HL, McGeehan JE, Beckham GT. 2018. Characterization and engineering of a plastic-degrading aromatic polyesterase. Proc Natl Acad Sci 115:E4350–E4357.

22. Son HF, Cho IJ, Joo S, Seo H, Sagong H-Y, Choi SY, Lee SY, Kim K-J. 2019. Rational Protein

Engineering of Thermo-Stable PETase from Ideonella sakaiensis for Highly Efficient PET Degradation. ACS Catal 9:3519–3526.

23. Cui Y, Chen Y, Liu X, Dong S, Tian Y, Qiao Y, Mitra R, Han J, Li C, Han X, Liu W, Chen Q, Wei W, Wang X, Du W, Tang S, Xiang H, Liu H, Liang Y, Houk KN, Wu B. 2021. Computational Redesign of a PETase for Plastic Biodegradation under Ambient Condition by the GRAPE Strategy. ACS Catal 11:1340–1350.

24. Bollinger A, Thies S, Knieps-Grünhagen E, Gertzen C, Kobus S, Höppner A, Ferrer M, Gohlke H, Smits SHJ, Jaeger K. 2020. A Novel Polyester Hydrolase From the Marine Bacterium Pseudomonas aestusnigri – Structural and Functional Insights. Front Microbiol 11.

25. Danso D, Schmeisser C, Chow J, Zimmermann W, Wei R, Leggewie C, Li X, Hazen T, Streit WR. 2018. New Insights into the Function and Global Distribution of Polyethylene Terephthalate (PET)-Degrading Bacteria and Enzymes in Marine and Terrestrial Metagenomes. Appl Environ Microbiol 84:e02773-17.

26. Gerday C, Aittaleb M, Arpigny JL, Baise E, Chessa JP, Garsoux G, Petrescu I, Feller G. 1997. Psychrophilic enzymes: a thermodynamic challenge. Biochim Biophys Acta 1342:119–31.

27. Yakimov MM, Giuliano L, Gentile G, Crisafi E, Chernikova TN, Abraham WR, Lünsdorf H, Timmis KN, Golyshin PN. 2003. Oleispira antarctica gen. nov., sp. nov., a novel hydrocarbonoclastic marine bacterium isolated from Antarctic coastal sea water. Int J Syst Evol Microbiol 53:779–785.

28. Feller G. 1990. Lipases from psychrotropic antarctic bacteria. FEMS Microbiol Lett 66:239–243.

29. Kube M, Chernikova TN, Al-Ramahi Y, Beloqui A, Lopez-Cortez N, Guazzaroni M-E, Heipieper HJ, Klages S, Kotsyurbenko OR, Langer I, Nechitaylo TY, Lünsdorf H, Fernández M, Juárez S, Ciordia S, Singer A, Kagan O, Egorova O, Petit PA, Stogios P, Kim Y, Tchigvintsev A, Flick R, Denaro R, Genovese M, Albar JP, Reva ON, Martínez-Gomariz M, Tran H, Ferrer M, Savchenko A, Yakunin AF, Yakimov MM, Golyshina O V, Reinhardt R, Golyshin PN. 2013. Genome sequence and functional genomic analysis of the oil-degrading bacterium Oleispira antarctica. Nat Commun 4:2156.

30. Schmidt J, Wei R, Oeser T, Belisário-Ferrari MR, Barth M, Then J, Zimmermann W. 2016. Effect of Tris, MOPS, and phosphate buffers on the hydrolysis of polyethylene terephthalate films by

polyester hydrolases. FEBS Open Bio 6:919–927.

31. Bartnikowski M, Dargaville TR, Ivanovski S, Hutmacher DW. 2019. Degradation mechanisms of polycaprolactone in the context of chemistry, geometry and environment. Prog Polym Sci 96:1–20.

32. Wei R, Oeser T, Then J, Kühn N, Barth M, Schmidt J, Zimmermann W. 2014. Functional characterization and structural modeling of synthetic polyester-degrading hydrolases from Thermomonospora curvata. AMB Express 4:44.

33. Leaver-Fay A, Tyka M, Lewis SM, Lange OF, Thompson J, Jacak R, Kaufman K, Renfrew PD, Smith CA, Sheffler W, Davis IW, Cooper S, Treuille A, Mandell DJ, Richter F, Ban YEA, Fleishman SJ, Corn JE, Kim DE, Lyskov S, Berrondo M, Mentzer S, Popović Z, Havranek JJ, Karanicolas J, Das R, Meiler J, Kortemme T, Gray JJ, Kuhlman B, Baker D, Bradley P. 2011. Rosetta3: An object-oriented software suite for the simulation and design of macromolecules. Methods Enzymol 487:545–574.

34. Kirley TL. 1989. Reduction and fluorescent labeling of cyst(e)ine-containing proteins for subsequent structural analyses. Anal Biochem 180:231–236.

35. Alcamán-Arias ME, Farías L, Verdugo J, Alarcón-Schumacher T, Díez B. 2018. Microbial activity during a coastal phytoplankton bloom on the Western Antarctic Peninsula in late summer. FEMS Microbiol Lett 365:fny090.

36. Bankevich A, Nurk S, Antipov D, Gurevich AA, Dvorkin M, Kulikov AS, Lesin VM, Nikolenko SI, Pham S, Prjibelski AD, Pyshkin A V, Sirotkin A V, Vyahhi N, Tesler G, Alekseyev MA, Pevzner PA. 2012. SPAdes: A New Genome Assembly Algorithm and Its Applications to Single-Cell Sequencing. J Comput Biol 19:455–477.

37. Hyatt D, Chen G-L, LoCascio PF, Land ML, Larimer FW, Hauser LJ. 2010. Prodigal: prokaryotic gene recognition and translation initiation site identification. BMC Bioinformatics 11:119.

38. Zhang Z, Schäffer AA, Miller W, Madden TL, Lipman DJ, Koonin E V, Altschul SF. 1998. Protein sequence similarity searches using patterns as seeds. Nucleic Acids Res 26:3986–3990.

39. Almagro Armenteros JJ, Tsirigos KD, Sønderby CK, Petersen TN, Winther O, Brunak S, von Heijne G, Nielsen H. 2019. SignalP 5.0 improves signal peptide predictions using deep neural networks. Nat Biotechnol 37:420–423.

40. Alarcón-Schumacher T, Guajardo-Leiva S, Antón J, Díez B. 2019. Elucidating Viral Communities During a Phytoplankton Bloom on the West Antarctic Peninsula. Front Microbiol 10:1014.

41. Langmead B, Salzberg SL. 2012. Fast gapped-read alignment with Bowtie 2. Nat Methods 9:357–359.

42. Nikolaivits E, Dimopoulou P, Maslak V, Nikodinovic-Runic J, Topakas E. 2020. Discovery and biochemical characterization of a novel polyesterase for the degradation of synthetic plastics. Chem Proc 2:33.

43. Santiago M, Ramírez-Sarmiento CA, Zamora RA, Parra LP. 2016. Discovery, Molecular Mechanisms, and Industrial Applications of Cold-Active Enzymes. Front Microbiol 7:1408.

44. Wei R, Song C, Gräsing D, Schneider T, Bielytskyi P, Böttcher D, Matysik J, Bornscheuer UT, Zimmermann W. 2019. Conformational fitting of a flexible oligomeric substrate does not explain the enzymatic PET degradation. Nat Commun 10:3–6.

45. Dong X, Xing T, Chen G. 2020. Improving the anti-pilling performance of cellulose fiber blended knitted fabrics with 2,4,6-trichloropyrimidine treatment. Coatings 10:1–16.

46. Meyer-Cifuentes IE, Werner J, Jehmlich N, Will SE, Neumann-Schaal M, Öztürk B. 2020. Synergistic biodegradation of aromatic-aliphatic copolyester plastic by a marine microbial consortium. Nat Commun 11:5790.

47. Magrane M, Consortium U. 2011. UniProt Knowledgebase: a hub of integrated protein data. Database 2011:bar009–bar009.

48. Ishida T, Kinoshita K. 2007. PrDOS: prediction of disordered protein regions from amino acid sequence. Nucleic Acids Res 35:W460–W464.

49. Bradford MM. 1976. A rapid and sensitive method for the quantitation of microgram quantities of protein utilizing the principle of protein-dye binding. Anal Biochem 72:248–254.

50. Stainmesse S, Orecchioni AM, Nakache E, Puisieux F, Fessi H. 1995. Formation and stabilization of a biodegradable polymeric colloidal suspension of nanoparticles. Colloid Polym Sci 273:505–511.

51. Belisário-Ferrari MR, Wei R, Schneider T, Honak A, Zimmermann W. 2019. Fast Turbidimetric Assay for Analyzing the Enzymatic Hydrolysis of Polyethylene Terephthalate Model Substrates.

Biotechnol J 14:1800272.

52. Wei R, Oeser T, Barth M, Weigl N, Lübs A, Schulz-Siegmund M, Hacker MC, Zimmermann W. 2014. Turbidimetric analysis of the enzymatic hydrolysis of polyethylene terephthalate nanoparticles. J Mol Catal B Enzym 103:72–78.

53. Palm GJ, Reisky L, Böttcher D, Müller H, Michels EAP, Walczak MC, Berndt L, Weiss MS, Bornscheuer UT, Weber G. 2019. Structure of the plastic-degrading Ideonella sakaiensis MHETase bound to a substrate. Nat Commun 10:1717.

54. Berman HM. 2000. The Protein Data Bank. Nucleic Acids Res 28:235–242.

55. Ribitsch D, Hromic A, Zitzenbacher S, Zartl B, Gamerith C, Pellis A, Jungbauer A, Łyskowski A, Steinkellner G, Gruber K, Tscheliessnig R, Herrero Acero E, Guebitz GM. 2017. Small cause, large effect: Structural characterization of cutinases from Thermobifida cellulosilytica. Biotechnol Bioeng 114:2481–2488.

56. Roth C, Wei R, Oeser T, Then J, Föllner C, Zimmermann W, Sträter N. 2014. Structural and functional studies on a thermostable polyethylene terephthalate degrading hydrolase from Thermobifida fusca. Appl Microbiol Biotechnol 98:7815–7823.

57. Bender BJ, Cisneros A, Duran AM, Finn JA, Fu D, Lokits AD, Mueller BK, Sangha AK, Sauer MF, Sevy AM, Sliwoski G, Sheehan JH, DiMaio F, Meiler J, Moretti R. 2016. Protocols for Molecular Modeling with Rosetta3 and RosettaScripts. Biochemistry 55:4748–4763.

58. Lüthy R, Bowie JU, Eisenberg D. 1992. Assessment of protein models with three-dimensional profiles. Nature 356:83–85.

59. Pontius J, Richelle J, Wodak SJ. 1996. Deviations from Standard Atomic Volumes as a Quality Measure for Protein Crystal Structures. J Mol Biol 264:121–136.

60. Laskowski RA, MacArthur MW, Moss DS, Thornton JM. 1993. PROCHECK: a program to check the stereochemical quality of protein structures. J Appl Crystallogr 26:283–291.

61. Hooft RWW, Vriend G, Sander C, Abola EE. 1996. Errors in protein structures. Nature 381:272–272.

62. Song Y, Dimaio F, Wang RYR, Kim D, Miles C, Brunette T, Thompson J, Baker D. 2013. High-resolution comparative modeling with RosettaCM. Structure 21:1735–1742.

63. Maier JA, Martinez C, Kasavajhala K, Wickstrom L, Hauser KE, Simmerling C. 2015. ff14SB: Improving the Accuracy of Protein Side Chain and Backbone Parameters from ff99SB. J Chem Theory Comput 11:3696–3713.

64. Anandakrishnan R, Aguilar B, Onufriev A V. 2012. H++ 3.0: automating pK prediction and the preparation of biomolecular structures for atomistic molecular modeling and simulations. Nucleic Acids Res 40:W537–W541.

65. Ryckaert JP, Ciccotti G, Berendsen HJC. 1977. Numerical integration of the cartesian equations of motion of a system with constraints: molecular dynamics of n-alkanes. J Comput Phys 23:327–341.

66. Darden T, York D, Pedersen L. 1993. Particle mesh Ewald: An N ·log(N) method for Ewald sums in large systems. J Chem Phys 98:10089–10092.

67. Roe DR, Cheatham TE. 2013. PTRAJ and CPPTRAJ: Software for processing and analysis of molecular dynamics trajectory data. J Chem Theory Comput 9:3084–3095.

68. Bengtsson-Palme J, Hartmann M, Eriksson KM, Pal C, Thorell K, Larsson DGJ, Nilsson RH. 2015. metaxa2: improved identification and taxonomic classification of small and large subunit rRNA in metagenomic data. Mol Ecol Resour 15:1403–1414.

FIGURE LEGENDS

Figure 1. Hydrolysis of PCL by Mors1 and OaCut. **(A)** Agar plate containing PCL with *E. coli* expressing Mors1. **(B)** Agar plate containing PCL with *E. coli* expressing OaCut. **(C)** Time course of PCL hydrolysis (decrease of turbidity of a PCL nanoparticle suspension) by Mors1 (blue) and OaCut (black). **(D)** Relative initial hydrolysis rates of PCL nanoparticles by Mors1 at different reaction temperatures; 100% = hydrolysis rate at 25°C. **(E)** Determination of the thermal inactivation temperature (T_{50} = 48.7°C) of Mors1.

Figure 2. **Enzymatic degradation of amorphous PET films. (A)** Weight loss of PET films (in dark green) and amounts of TPA and MHET (in pink) released by Mors1 and *Is*PETase after a reaction time of 24h at 25°C. In grey, negative control without enzyme. **(B)** Weight loss of PET films after a reaction time of 6 days at 25°C with Mors1 and OaCut. NC: Negative control without enzyme. **(C)** Weight loss of PET films after a reaction time of 1, 7, and 10 days at 25°C with Mors1. **(D)** Surface changes of amorphous PET films. Control (left) and treated with Mors1 for 10 days at 25°C (right)**.** Scanning electron microscopic images of the surface of an untreated PET film (**E**) and a film treated with Mors1 for 10 days at 25°C **(F)**.

Figure 3. Comparison of the sequence, structure, and active site dynamics of Mors1, OaCut, *Is*PETase, *Tf*Cut2, and LCC. (**A**) Multiple sequence alignment. Residues numbered according to the full protein sequences with signal peptide. Strictly conserved residues are highlighted in green background, with yellow triangles indicating cysteine pairs that form disulfide bonds and orange stars indicating catalytic residues. A secondary structure topology

based on the structure of *Tf*Cut2 (PDB 4CG1) is shown on top of the sequence alignment. (**B**) Cartoon representation of the modelled structure of Mors1, showing its three disulfide bridges (DB) in yellow sticks. (**C**) Active site of Mors1 (blue), with catalytic residues in bold. (**D**) Active site of *Is*PETase (green), showing residues equivalent to Mors1 and catalytic residues in bold. (**E**) Average backbone RMSF for Mors1 and *Is*PETase. The secondary structure is indicated as lines in the background, with α-helices in pink and β-sheets in grey.

Figure 4. Sequence variability of potential polyester hydrolases from Antarctic metagenomes. A multiple sequence alignment between Mors1 and homologous enzyme candidates with high sequence coverage from Antarctic metagenomes from Chile Bay. Blue boxes indicate columns with either strict (red background) or 75% (red characters) sequence conservation between all enzymes. Green stars indicate conserved catalytic residues, whereas blue spheres indicate active site residues.

782 **TABLES**

783

784 **Table 1.** Onset temperature for denaturation and melting temperature (Tm) of Mors1, OaCut and

785 *Is*PETase determined with nanoDSF.

	Onset temperature for denaturation (ºC)	T_m (ºC)
Mors1	31.0 ± 0.0	52.0 ± 0.1
OaCut	34.8 ± 0.3	40.4 ± 0.1
*Is*PETase	31.7 ± 0.3	47.1 ± 0.3

786

787 **Table 2.** Kinetic parameters of PCL hydrolysis by Mors1, *Is*PETase, Tcur1278 and Tcur0990.

	k_τ (10^{-3}/min^{-1})	K_A (ml/mg)
Mors1	1544 ± 23	152 ± 5
*Is*PETase	1688 ± 81	94 ± 8
Tcur1278	122 ± 12	41 ± 5
Tcur0390	108 ± 6	96 ± 10

788

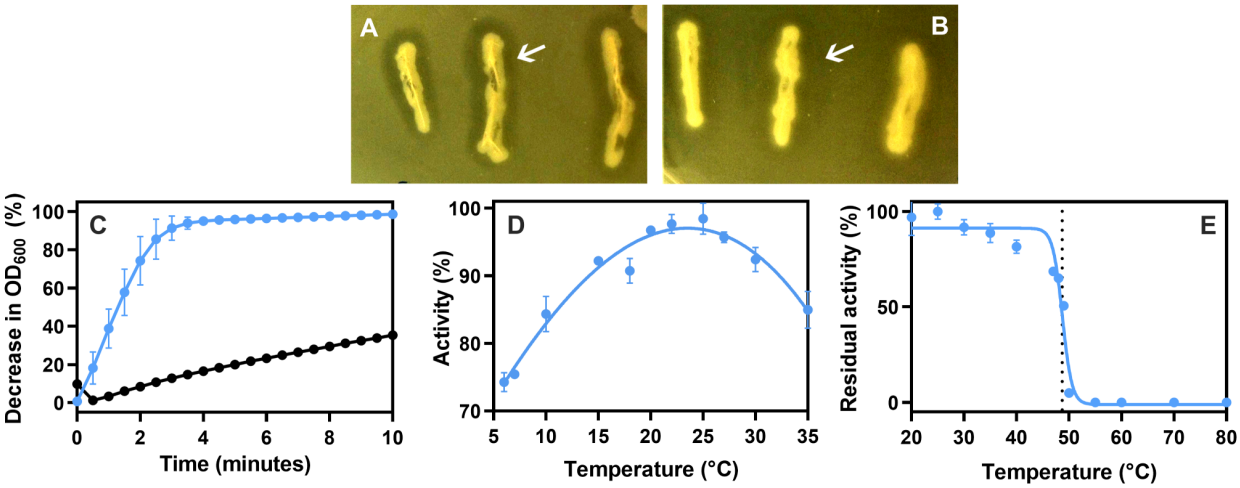

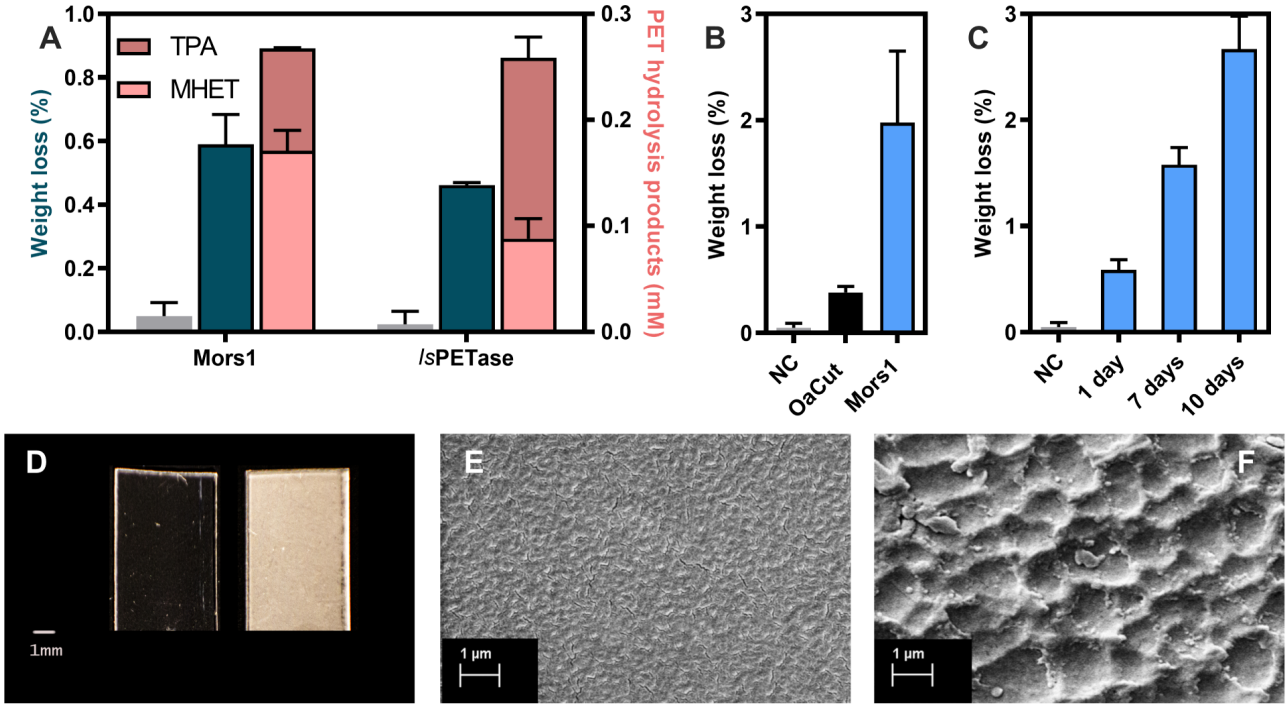

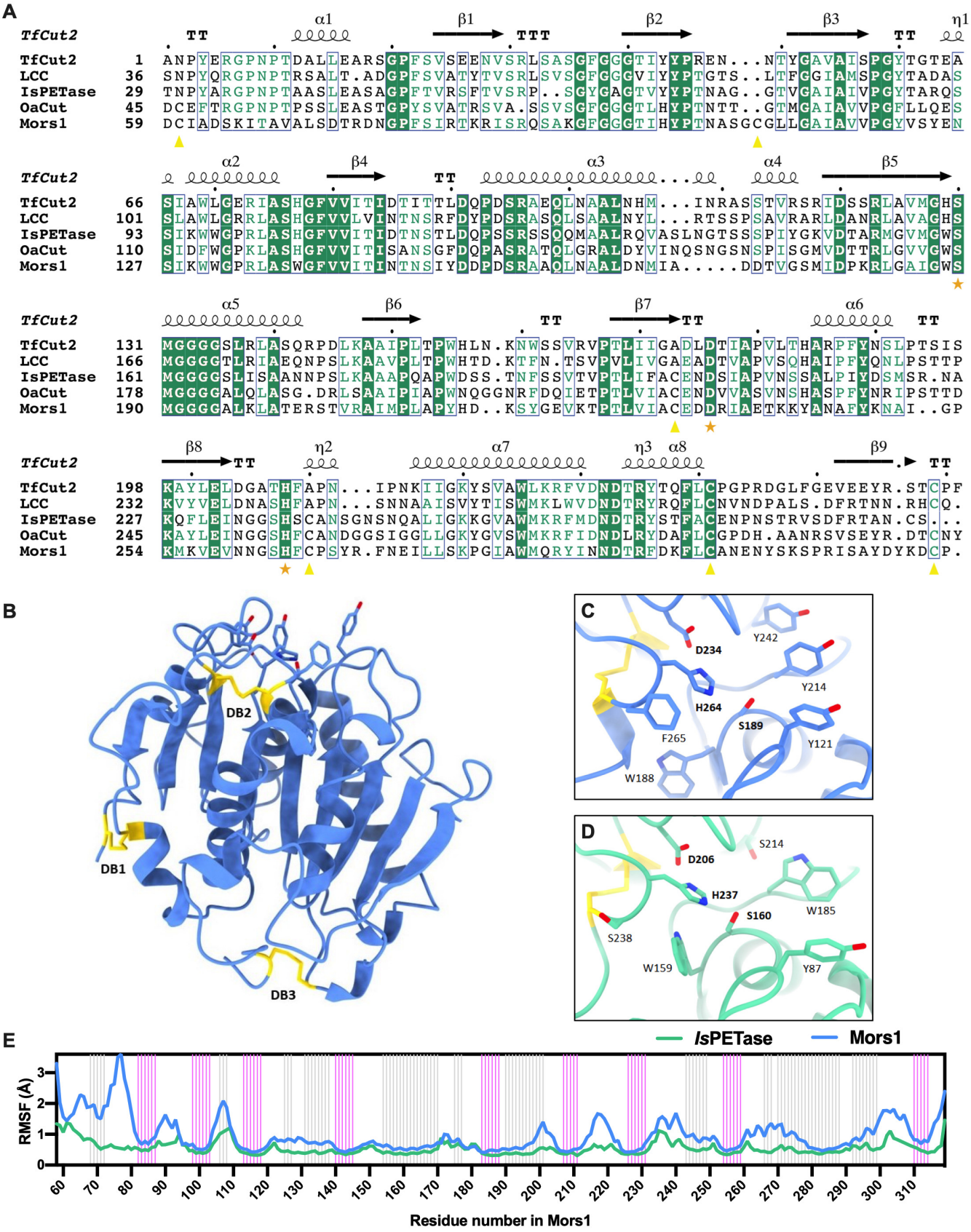

```
         60        70        80        90       100       110       120       130       140
Mors1    DCIADSKITAVALSDTRDNGPFSIRTKRISRQSAKGFGGGTIHYPTNASGCGLLGAIAVWPGYVSYENSIKWWGPRLASWGFVVITINTN
mtgnm2   .......ITAAALSDTRDNGPFSVSTKHVARQSAKGFGGGTIHYPTDAIGCGLLGAIAVWPGYVSYEAAIKWWGPRLASWGFVVITIDTN
mtgnm4   DCIADSAITADALSDTRNNGPFSVRTKRVSRQSAKGFGGGTIHYPTNASGCGLLGAIAVWPGYVSYEAAIKWWGPRLASWGFVVITINTH
mtgnm5   ....SSDVCSSDLSDTRDKGPFSVAKKAVPRQLAKGFGGGTIYYPTNAGGCGLLGGIAVIPGYVSYESSIKWWGPRLASWGFVVITIDTN
mtgnm6   NCIADSAITAAALSDTRDNGPFSVSTKHVARQSAKGFGGGTIHYPTDAIGCGLLGAIAVWPGYVSYEAAIKWWGPRLASWGFVVITIDTN

        150       160       170       180       190       200       210       220       230
Mors1    SIYDDPDSRAAQLNAALDNMIADDTVGSMIDPKRLGAIGWSMGGGGALKLATERSTVRAIMPLAPYHDKSYGEVKTPTLVIACEDDRIAE
mtgnm2   SIYDDPNSRATQLNAALDHIIADDTVGNKIDPKRLGAIGWSMGGGGALKLAKERSTVRAIMPLAPYHDKSYGEVKTPTLVIACERDRIAT
mtgnm4   SIYDDPDSRAAQLNAALDHMIADDTVGSMIDPTRLGAIGWSMGGGGALRLATERSTVRAIMPLAPYHNKSYGAVKTPTLVITCEHDRIAS
mtgnm5   SIYDDPESRAAQLSAALYHMLRDNTVGAQIDSTRLGAIGWSMGGGGALQLATKRQTVRAIIPQTPYHDKDYGEMNTPALFITCQNDRIAS
mtgnm6   SIYDDPNSRATQLNAALDHIIADDTVGNKIDPKRLGAIGWSMGGGGALKLAKERSTVRAIMPLAPYHDKSYGEVKTPTLVIACERDRIAT

        240       250       260       270       280       290       300       310
Mors1    TKKYANAFYKNAIGPKMKVEVNNGSHFCPSYRFNEILLSKPGIAWMQRYINNDTRFDKFLCANENYSKSPRISAYDYKDCP
mtgnm2   NEKYTNVFYHNATGPKMKIEVDNGSHFCPTYRFNEILLSKPGIAWMQRYINNDTRFDKFLCANENYSKSPRISAYDYKDCS
mtgnm4   NNKYSNAFYKNATGPKMIVEVNNGSHFCPSYRFNEILLSKPGIAWMQRHINNDTRFDKFLCANENYSKSPRISAYNYKDCP
mtgnm5   NKKYSSRFYDKATGAKMKIEIKNGSHFCPSYRFNEILLSKPGIAWMHRYINGDIRFNQFLCSNDNYGNNPRISAYDYKNCS
mtgnm6   NEKYTNVFYHNATGPKMKIEVDNGSHFCPTYRFNEILLSKPGIAWMQRYINNDTRFDKFLCANENY...........
```